Adjustable polysaccharides-proteins films made of aqueous wheat proteins and alginate solutions

Bishnoi, Shahana; Trifol, Jon; Moriana, Rosana; Mendes, Ana C.

Published in:
Food Chemistry

Link to article, DOI:
10.1016/j.foodchem.2022.133196

Publication date:
2022

Document Version
Publisher's PDF, also known as Version of record

Food Chemistry 391 (2022) 133196

Contents lists available at ScienceDirect

Food Chemistry

journal homepage: www.elsevier.com/locate/foodchem

Adjustable polysaccharides-proteins films made of aqueous wheat proteins and alginate solutions

Shahana Bishnoi [a], Jon Trifol [b,c], Rosana Moriana [b], Ana C. Mendes [a,*]

[a] DTU-Food, Technical University of Denmark (DTU) 202, 2800Kgs Lyngby, Denmark
[b] KTH Royal Institute of Technology, Stockholm, Sweden
[c] Department of Chemical and Metallurgical Engineering, School of Chemical Engineering, Aalto University, P.O. Box 16300, FIN-00076 Aalto, Espoo, Finland

ARTICLE INFO

Keywords:
Edible films
Food packaging
Food coatings
Wheat proteins
Alginate

ABSTRACT

Large amount of wheat proteins by-products are produced during wheat starch manufacture. This work aimed to develop edible films of cast aqueous wheat proteins (WP) and alginate (Al) solutions. The investigation of the microstructure of Al/WP films revealed a more compacted cross-section and homogeneous surface, comparatively to Al films. Those properties could be modified with the increase of WP concentration from 4 to 8 % w/v, as result of electrostatic interactions between WP and Al. Furthermore, the incorporation of WP provided UltraViolet-blocking behaviour (4-fold decrease in the Ultra-Violet-B region). Additionally, the incorporation of WP in the films reduced the water solubility of the Al films. It was also found that by incorporating different amounts of WP the mechanical and Water Vapor Transmission rate (WVTR) properties could also be modified, so the film composition could be adjusted to suit different types of foods and applications (e.g. coatings and packaging).

1. Introduction

The demand for new edible films, structures made of food-grade components (e.g. proteins, polysaccharides and lipids), have been growing in the past years. An edible film is defined as a material with a thickness of<0.3 mm, which is formed from a combination of biopolymers and different additives, dispersed in aqueous media (Diaz-Montes & Castro-Muñoz, 2021). Edible films can be applied as coats on the food surface, between food components, and/or sealed into edible bags (Otoni et al., 2017).They can improve the sensory properties of foods (e.g. taste trough the texture and the appearance) (Pascall & Lin, 2013). Other applications include the immobilization of minerals and bioactive compounds, such as vitamins, anti-oxidants, probiotics, which tend to improve the nutritional value of the foods as well as the healthy benefits for the consumer (Pascall & Lin, 2013). Additionally, they have been also used in packaging applications to improve the shelf-life of the food products through its protection against external agents such as gases, moisture, mechanical stress or microbial contamination (Otoni et al., 2017). Edible films are often made of biodegradable biopolymeric materials, which can be more environmentally friendly than their fossil-based materials counterparts (Pascall & Lin, 2013), and significantly reduce the negative climate impacts (Mendes & Pedersen, 2021).

Specifically, edible films made of polysaccharides and proteins have been gaining interest (Rojas-Lema et al., 2021), as most of those biopolymers can have good film forming properties, mainly due to their functional chemical groups and polyelectrolyte nature.

Overall, polysaccharides are abundant in nature, affordable, nontoxic (Mohamed et al., 2020) and resistant to high temperatures. Polysaccharide-based edible films are known for being chemically stable and can be designed to afford long-term storage with suitable physical, mechanical (Mohamed et al., 2020; Zhang et al., 2019), and gas barrier properties(Pascall & Lin, 2013; Parreidt et al., 2018; Jon Trifol et al., 2021). Alginates are anionic polysaccharides, extracted mainly from brown seaweeds, comprising in their molecular structure combinations of β-D-mannuronic acid (M) and α-L-guluronic acid (G) linked by 1–4 glycosidic bonds (Parreidt et al., 2018; Comaposada et al., 2015; Rhim, 2004; Barbut & Harper, 2019; Silva et al., 2009). Due to the propensity to dissolve in water and lower mechanical properties, usually alginate films are produced by crosslinking alginates with di- or tri-valent ions (e.g. Ca^{2+}) (Parreidt et al., 2018; Rhim, 2004), and/or positively charged macromolecules (e.g. chitosan), (Comaposada et al., 2015). The interest on alginate-based edible films has been increasing, as alginate-based salts are an authorized food additive, non-expensive and can form uniform, thermo-irreversible and water low solubility gels. The

* Corresponding author.
E-mail address: anac@food.dtu.dk (A.C. Mendes).

https://doi.org/10.1016/j.foodchem.2022.133196
Received 11 November 2021; Received in revised form 28 April 2022; Accepted 8 May 2022
Available online 13 May 2022

physicochemical and mechanical properties of the alginate-based films are dependent on the composition and the gelation method. Thus, crosslinked alginate edible films properties have been tailored to enhance the shelf-life of fresh-cut fruits and vegetables, meat, poultry, and cheese products (Parreidt et al., 2018). However, if not crosslinked, like with most of the polysaccharides based films, alginate films have low moisture barrier properties(Pascall & Lin, 2013) and dissolve faster under aqueous environments (Mendes & Pedersen, 2021).

Proteins, which have been widely used in edible packaging, have been proved for higher moisture resistance and mechanical properties, comparatively to polysaccharides films, (Mendes & Pedersen, 2021; Parreidt et al., 2018). Furthermore, protein edible films can provide additional nutritional value and improved sensory properties to the foods (Zhang et al., 2019).

Wheat gluten proteins, which consists of mixtures of gliadin and glutenin protein subunits (Garg et al., 2019), have been used in bakery industry to enrich flours for bread and pasta (Skendi et al., 2020), and in the production animal feeds, adhesives (Day et al., 2006) and bioplastics (Langstraat et al., 2015). Yet, a large amount of wheat proteins by-products are produced during wheat starch manufacture, and therefore the valorization and usage of those proteins is still emergent in the cereal processing industry (Skendi et al., 2020). Wheat proteins can also be used to make functional films with tuned mechanical and oxygen barrier properties, which might find applications in coatings and packaging (Mojumdar et al., 2011) for several industries, including food. Overall wheat gluten proteins are insoluble in water, and consequently it is necessary a complex solvent system with basic or acidic conditions in the presence of alcohol and disulfide bond-reducing agents (Buffo & Han, 2005). Individual wheat proteins films have been produced by dispersing the proteins in organic solvents such as absolute ethanol (Ali et al., 1997), acetic acid (Gontard et al., 1993) and mixtures of ethanol/water (Mojumdar et al., 2011) followed by protein denaturation at 70–75 ℃ prior casting in a mold. The fact that wheat proteins films have been produced using organic solvents, have been limiting the use of these proteins in applications and industries (e.g. food) that require "greener" and alcohol-free methodologies for product development and further commercialization to wider markets (e.g. Halal foods). Furthermore, edible films require the dispersion of the food grade ingredients in aqueous media, to be classified as edible films (Diaz-Montes & Castro-Muñoz, 2021).

In recent years, composite edible films made of combinations polysaccharides and proteins, have shown superior properties (e.g. water resistance and mechanical) than films made of individual polysaccharides and proteins, as confirmed in the characterization of rapeseed protein hydrolysate-chitosan (Zhang et al., 2019) and whey protein isolate-fructan films (Mozafarpour et al., 2021).

Herein, wheat proteins/alginate edible films were produced, to potentiate the valorization and usage of wheat proteins, one of the major by-products of wheat starch manufacture. In this study, we hypothesized that by combining aqueous wheat proteins and alginate solutions, alginate/wheat proteins (Al/WP) edible films could be produced, using a "greener" approach (without the use of organic solvents). Furthermore, the Al/WP films properties could be adjusted to match the requirements of a specific application. To this end, the effect of the pH on wheat proteins solutions and interactions with alginate (in solution) were investigated to improve the film forming properties. The effect of the concentration of wheat proteins on the Al/WP films properties (microstructure, thickness, color, mechanical properties, water solubility and vapor permeability) were also investigated and compared with individual alginate films.

2. Materials and methods

2.1. Materials

Wheat proteins (Nutralys W, CAS no 100684–25-1) was kindly supplied by Roquette (Lestrem, France). Sodium Alginate (W201502, Lot #MKCC4541) and all the chemicals were purchased from Sigma-Aldrich Co., Ltd., (St. Louis, Missouri, United States), unless otherwise indicated. The chemicals were used as received.

2.2. Preparation of alginate and protein solutions

Aqueous Alginate solution (Al) were prepared by mixing 2 %.w/v of sodium alginate in ultrapure water (Milli-Q® Integral Water Purification System for Ultrapure Water (MilliporeSigma, Merck Group, Burlington, Massachusetts) with 1 %. w/v glycerol (Rhim, 2004). Aqueous wheat proteins (WP) solutions were prepared by dispersing 4, 6 and 8 %.w/v of wheat proteins in ultrapure water with 4 %.w/v glycerol (WP4, WP6 and WP8, respectively). Each of the aforementioned solutions were stirred at 600 rpm at room temperature (22 °C) until homogenous solutions were obtained. The solutions were thereafter stored at 4 °C.

2.3. Alginate-Protein interactions in solution

To predict alginate-protein interactions, turbidity and zeta potential measurements were conducted (Mendes et al., 2018). To conduct this study, WP solutions were prepared at the concentration of 4%.w/v, as this was the lowest concentration that allowed film formation with suitable properties. Therefore, Al and 4%.w/v of WP solutions previously described were prepared, and the pH of WP solutions was adjusted to 3, 7 and 10.

Samples were diluted with ultrapure water to a dilution factor of 4, prior analysis.

2.3.1. Turbidity

Al solution was mixed with WP solutions at pH 3 (3WP), pH 7 (7WP), pH 10 (10WP), in a proportion 1:1 (v:v), in a 96 well plate with a final volume of 200 μL in each well. The individual components (individual solutions of Al and WP) were also transferred to the well plate to be used as controls. Samples were incubated for 1 h at room temperature (22 °C). Turbidity profiles of alginate, protein, mixtures of alginate-protein were assessed by the changes in absorbance at the wavelength of 620 nm in an EnSpire Multimode Plate Reader (PerkinElmer, Skovlunde, Denmark), and turbidity was calculated using the following equation:

$$Turbidity = (2.3*A)/L$$

derived from Beer-lambert's law, where A is the absorbance and L is the optical path length. These studies were conducted in triplicate for each condition (N = 3).

2.3.2. Zeta potential

Zeta potential was determined by collecting 50 μL of the sample from the 96-well plate prepared in section 2.3.1, in addition to 950 μL of ultrapure water. The solutions were homogenized by gently pipetting prior Zeta potential measurements using a Malvern Zetasizer NanoZS (Malvern Instruments, Worcestershire, UK). Zeta potential was measured by mixed laser Doppler electrophoresis and phase analysis light scattering. These studies were conducted in triplicate for each condition (N = 3).

2.4. Preparation of the Alginate-Protein films

Films were prepared by solvent casting mixtures of the alginate and protein solutions in a 1:1 (v:v) ratio at pH 4(Z. Zhang et al., 2016). The mixture was magnetically stirred at 600 rpm at room temperature (22 °C) for 15 min prior to being cast into 15 mm polystyrene petri dish. The film formation was accelerated by drying it in a Memmert hot air oven (Buch & Holm A/S, Herlev, Denmark) at 60 °C for 18 h. The resultant films were peeled manually from the surface of the petri dish for further characterization.

2.5. Characterization of Alginate-Protein films

2.5.1. Fourier transform infrared spectroscopy (FTIR)

To investigate alginate-protein interactions in the film, FTIR was used to assess the chemical structure of the individual alginate, protein and the alginate-protein complexes in the films. All the films were dried, crushed and placed in the sample holder to be analysed using a Spectrum 100 Optica FTIR spectrometer (PerkinElmer, Skovlunde, Denmark). Scans were made in the range of 515 to 4000 cm^{-1}.

2.5.2. Scanning electron microscopy (SEM)

The nano-micro structure of the films was analysed by Scanning electron microscopy (SEM). Samples stored in a desiccator were transferred to metal stubs with double-sided adhesive carbon tape (sample holder). To visualize the films cross section, films were cut with a scalpel and positioned in the sample holder. The samples were further sputter-coated with a 6 nm layer of gold (Leica Coater ACE 200, Leica, Vienna, Austria) prior to their imaging in a Quanta FEG 3D (FEI, Eindhoven, The Netherlands) scanning electron microscope.

2.5.3. X-Ray diffraction (XRD)

X-Ray Diffraction (XRD) patterns of the samples were obtained by using a Bruker CCD-Apex (Bruker, MA, US) apparatus equipped with an X-ray generator (Ni-filtered Cu-Ka radiation). The instrument was operated at 40 kV and 40 mA in a 2θ rage of 5°-50° with a 0.06° step.

2.5.4. Film thickness

Thickness of each of the films prepared was analysed using a Mitutoyo micrometer calliper (Mitutoyo Corporation, Takatsu-ku, Kawasaki, Japan) across three points of a rectangular cross-section of the film.

2.5.5. Colorimetric analysis

The films were placed on a standard colour plate provided by Konica Minolta and the color parameters were measured using a Konica Minolta Chroma meter CR-300 colorimeter (Konica Minolta Inc., Tokyo, Japan). L, a and b values are expressed as a difference of the measured and standard values described (Rhim, 2004), along with total colour difference (ΔE) calculated using the following equations:

$$L = L_{measured} - L^*$$

$$a = a_{measured} - a^*$$

$$b = b_{measured} - b^*$$

$$\Delta E = \left((L^* - L)^2 - -(a^* - a)^2 - -(b^* - b)^2\right)^{1/2}$$

where, L*, a* and b* are the colour values of the standard plate and (L, a and b) measured are the values recorded of the film when placed on the standard colour plate.

L indicates lightness (0–100) with 0 being black and 100 being white. a indicates red if (+) and green if (−); b indicates yellow if (+) and blue if (−). The limits for a and b are approximately + or – 80 (Wrolstad & Smith, 2017).

2.5.6. UV–Vis spectroscopy

The UV– Vis absorption spectra was measured in the range of 190–800 nm for each film with a NanoDrop One UV–Vis spectrophotometer, Thermo Fisher Scientific (Massachusetts, United States). The transparency (T) of the films was determined following the equation:

$$T = -\frac{Log(T600)}{t}$$

where T is the fractional transmittance at 600 nm, and t is the film thickness (mm) (Kaewprachu et al., 2016).

2.5.7. Water solubility (WS)

Films sections of 1 cm × 1 cm were cut and placed in 5 mL of milliQ water at room temperature (22 °C) and at 90 °C, in a water bath (Julabo SW22, Seelbach, Germany), with gentle stirring at 40 rpm. After 1 h, the samples were observed and classified either as soluble, partially soluble or insoluble in water.

2.5.8. Water vapour transmission rate (WVTR)

The WVTR of the films was measured in triplicate at 23 °C and 50% RH by using the cup method. Briefly, a desiccating agent (calcium chloride) was placed inside a cup. Then the cup was hermetically sealed with the test film, and placed under controlled atmosphere (23 °C and 50% RH). Then the mass of the cup was weighted every hour, the mass increase of the cup was plotted versus time and the slope (n, g/day) was calculated. The WVTR was calculated using the following equation, where S is the cross section of the cup (5 cm^2) and l the film thickness (mm).

$$WVTR = n^*\frac{l}{S}$$

Finally, the WVTR of the materials was then divided by 100 (mm) to obtain the WVTR of a 100 mm film (Jon Trifol et al., 2021).

2.5.9. Mechanical properties

The tensile properties of the films, tensile strength, elastic modulus and the % elongation at break were determined by the use of a TA.XT plus Texture Analyser (Stable Micro Systems Ltd.,Surrey, United Kingdom) under a tension mode. Each of the films were cut into cross-section of 1.27 X 5 cm. The specimens were clamped in tensile grips for the analysis. The texture analyser yields data for the force (N) as a function of distance (mm) which was used to plot the stress–strain curves and obtain values for the various tensile properties. Each film was measured at least three times and then averaged.

2.6. Statistical analysis

Student's T-test was applied to determine statistical significance using Excel software (Microsoft corporation 2016). One-tailed unpaired t-test with 95% confidence interval was considered statistically significant if $P < 0.05$ (*), $P < 0.01$ (**) and $P < 0.001$ (***).

3. Results and *discussion*

3.1. Alginate-Protein interactions in solution

The effect of the pH on the alginate-protein interactions was investigated by turbidity and zeta potential of the individual biopolymers and mixtures (Fig. 1). Alginate solutions displayed very low absorption (0.2 cm^{-1}) comparatively to the proteins solutions (Fig. 1A). The turbidity of the individual protein solutions ranged from 0.5 to 1 cm^{-1} at the different pH tested. After mixing alginate with wheat proteins, only at pH 3, an abrupt increase in turbidity ($P < 0.001$) to 2.45 cm^{-1} was observed (Fig. 1A). This could be attributed to the formation of complexes between the negatively charged alginate and positively charged wheat proteins (at pH3). The mixtures formed at pH7 and pH10 did not show significant differences comparatively to the individual protein solutions (about 1 cm^{-1} for pH 7 and about 0.5 cm^{-1} for pH 10).

Fig. 1B confirms the polyanionic nature of alginate with a negative zeta potential (-34 mV). At pH 3, wheat proteins displayed a zeta potential of + 25.5 mV, probably due to the protonated carboxylate groups (−COOH) and the ionized amine groups ($-NH3^+$) on wheat proteins. However, when increasing the pH to 7 and 10, the zeta potential changed to −7.9 and –23.2 mV, respectively ($P < 0.01$), probably due to ionization of carboxylate and protonation of amine groups post isoelectric point (around pH 7–8 (Mojumdar et al., 2011)). After adding alginate to wheat proteins solutions, the zeta potential increased to

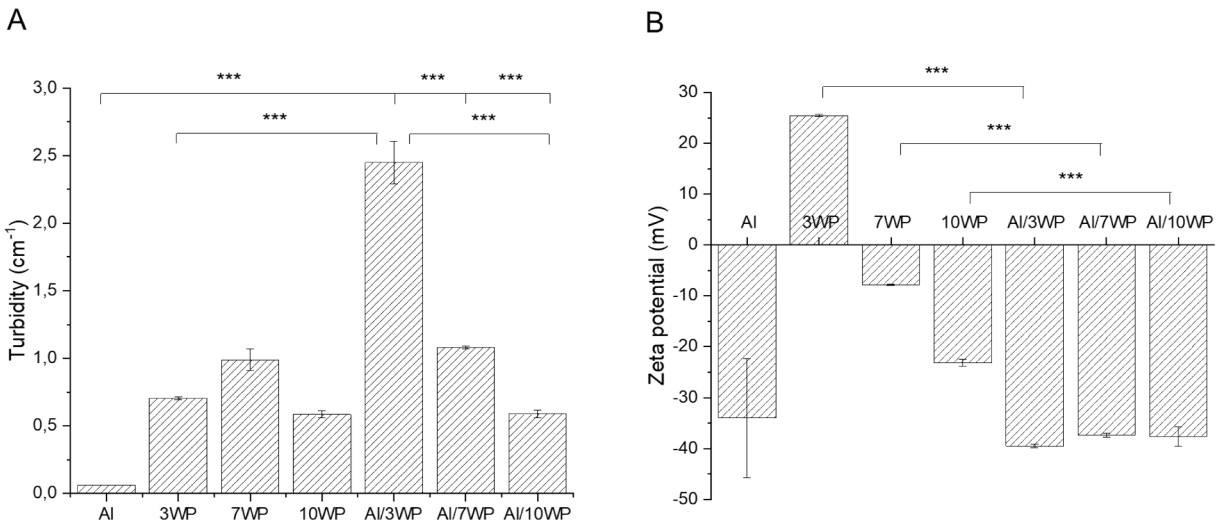

Fig. 1. Turbidity (A), and zeta potential (B) of the individual Al and Al/WP mixtures solutions at pH of 3 (Al/3WP), 7(Al/7WP) and 10 (Al/10WP). (N = 3).

−39.5; −37.4 and −37.7 mV for wheat proteins at pH 3 (3WP), 7(7WP), and 10(10WP), respectively. The increase in zeta potential for Al/WP solutions, was statistically significant for all the wheat proteins solutions tested ($P < 0.001$), suggesting that the individual protein solutions were stabilized with the addition of alginate. Values of zeta potential above ± 30 mV have been considered a sign of stability against aggregation due to charge stabilization(Lowry et al., 2016). Furthermore, acidic wheat proteins solutions, at pH below isoelectric point are expected to favor the protein solubility and the film forming process(Mojumdar et al., 2011).

The complex formation between positively charged Whey Protein Isolate (WPI) and negatively charged alginate resulted also in a negatively charged complex as reported by Zhang *et al.*(Z. Zhang et al., 2016), due to the charge dominance of the anionic alginate molecules. Herein, the polysaccharides might prevent the formation of a compact protein layer at the air/water interface due to electrostatic repulsion, which increases the net negative charge of the complexes. When the charge density is sufficient, the polysaccharides may enhance the cohesion between complexes within the adsorbed layer, being the charge density of the polysaccharides dominant (Ganzevles et al., 2007).

Turbidity and zeta potential results suggested that Al/WP films could be produced through electrostatic interactions by casting the negatively charged Al with the positively charged WP solutions at acidic pH.

3.2. Characterization of the films

3.2.1. Alginate-protein interactions in the film (FTIR)

Fig. 2 shows FTIR spectra of alginate Al and the Al/WP films at WP concentration of 4 and 8 % w/v. Alginate films reveal the typical main bands from alginate at 3272 cm^{-1} due to –OH stretching, and at 1600 cm^{-1} and 1400 cm^{-1} due to the asymmetric and symmetric stretching of COO^-, respectively. Other relevant vibration peaks around 1026 cm^{-1} were mainly attributed to C—O—C stretch.

Typically wheat films (made out of organic solvents), would display a set of characteristic bands in the vicinity of 1650 cm^{-1}, and 1541–1543 cm^{-1}characteristic of amide-I and the amide-II regions, as reported elsewhere (Mojumdar et al., 2011). However, in our study, we could not produce single wheat films following the methodology described (using water as the solvent). Only with alginate, Al/WP films could be produced. In Al/WP films, the appearance of a band at 1544 cm^{-1}, which became broader for higher concentrations of the proteins, was noticed due to amide groups of the proteins. The addition of WP to alginate films also resulted in the shift of the band at 3272 cm^{-1} to a slightly higher wavenumber and became less broad, particularly for the concentration of WP of 8% that appear at 3289 cm^{-1}. Furthermore, the bands attributed to alginate COO^- stretching at 1600 cm^{-1} and 1400 cm^{-1} also shifted to higher wavelengths (1622 and 1411 cm^{-1}, respectively). This data confirms the ionic and electrostatic interactions between the carboxylic groups of alginate and the WP amide groups, along with hydrogen bonds to form the films, which probably can be stronger for the highest concentrations of WP. Similar effects were seen in FTIR of films made by ionic complexation of polyanionic alginate (negatively charged) with the positively charged chitosan (Salama et al., 2018).

3.2.2. Microstructure

Fig. 3 shows the microstructure of the films analysed by SEM. Alginate films display a more porous cross section, in comparison to Al/WP films. However, with the increase of proteins concentration, the films became more compact on their cross section and their surfaces more homogeneous.

The more compacted cross-sections and homogeneous surfaces of Al/WP films, in comparison to the Al films, suggests that the interactions Al-WP could confer improved structural integrity and stability to the Al films.

3.2.3. Crystallinity

Fig. 4A shows the XRD patterns of the Al and Al/WP films. Alginate films displayed very low intensity spectra, with two peaks at $2\theta = 15°$ and $2\theta = 24°$, as reported (Tong et al., 2017).

The XRD patterns of the Al/WP films shows two small diffraction peaks at $2\theta = 10°$ and $2\theta = 20°$, (Liu & Ma, 2016). No major differences are observed among the XRD patterns of Al/WP and alginate films.

3.2.4. Thickness

In this study individual alginate films displayed a thickness of 0.048 mm (Table 1), which is in the range of other alginate films reported (thickness ranging from 0.045 to 0.075 mm (Silva et al., 2009)). The addition of wheat proteins increased the thickness of the films ($P < 0.01$) comparatively to alginate films. However, when increasing gradually the protein concentration, the film thickness gradually decreased (not statistically significant) from 0.162 to 0.143 and ultimately to 0.136 mm, for Al/WP4, Al/WP6 and Al/WP8, respectively. AL/WP8 films thickness was statistically significantly lower than AL/WP4, due to the stronger interactions of the Al with the WP at higher WP concentrations (FTIR, Fig. 2), which tend to create more compact films in their cross section (SEM, Fig. 3). Biopolymers interactions have been show to influence the film thickness (Chakravartula et al., 2019).

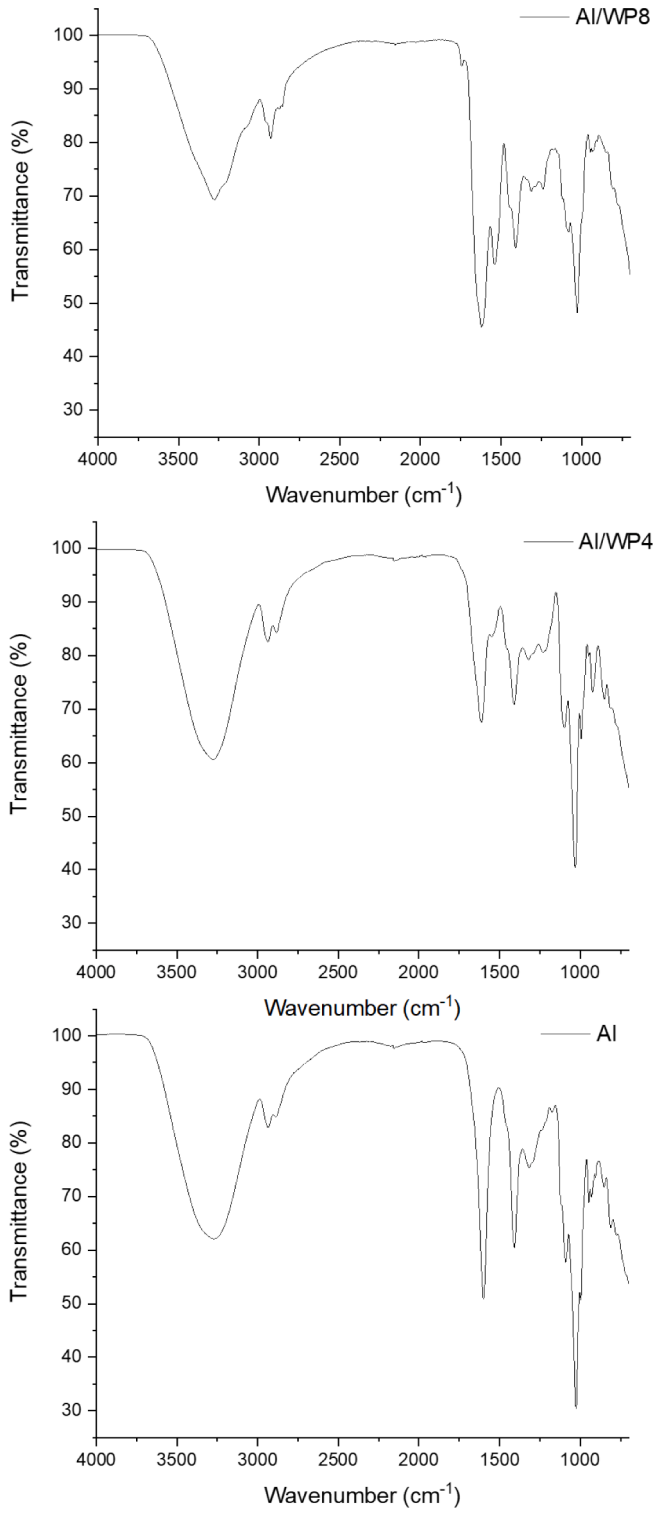

Fig. 2. FTIR spectra of Al, AL/WP4 and Al/WP6 films. (N = 3).

3.2.5. *Optical properties*

Color parameters (L, a, b and ΔE) are displayed in Table 1. Alginate films (control) displayed L = −0.97, a = 0,08, b = 1.84, and ΔE = 2.11. Al/WP films containing 4% of proteins did not change significantly those values ($P > 0.05$). However, for Al/WP6, the b and ΔE increased significantly ($P < 0.01$) to 9.25 and 9.92 respectively, while L and a decreased to −3.41 and −0.9 respectively. Samples acquired a darker yellowish values (higher b) for higher amounts of protein (above 6%.w/v). The increase in b values and decrease in L values have been associated with the increase of protein concentration, as reported in other protein based films (Chinabhark et al., 2007; Kaewprachu et al., 2016). The changes in color parameters of Al/WP8, were not significantly different comparatively to Al/WP6 films ($P > 0.05$).

UV–Vis analysis were performed to investigate transparency and light transmission in UV and visible ranges (Fig. 4B). Alginate films were transparent, and the additions of WP decreased significantly ($P < 0.01$) the transparency (Table 1). The decrease on transparency upon the addition of proteins to other polysaccharide matrices could be the result of interactions between components and network re-arrangements (Chakravartula et al., 2019). In the UV range, Al films seem to have a distinct absorption band around 213 nm and little absorption for the other wavelengths. On the other hand, Al/WP films absorb more on the UV area than Al films with consequent less transmittance, which suggest UV-blocking behaviour. Al has a transmittance in the UV-A (350 nm), UV-B (300 nm), UV-C (200 nm) of 84%, 77%, and 15%, respectively, while Al/WP8 has a transmittance of 48%, 20% and 23%. The incorporation or proteins provided UV-blocking behaviour to the Al films, especially in the UV-B region where the transmittance is decreased by 4 folds. This is important as the UV-light is known to decrease the shelf-life of some foods (J. Trifol et al., 2019), by degrading some proteins (Csapó et al., 2019), which can also affect the sensory properties of foods. Therefore, the films presented in this study can be tuned to be used in applications where UV light degrades food (e.g. food packaging).

3.2.6. *Water solubility (WS)*

The solubility of Al and Al/WP films with different protein concentrations is shown in the Table 2. From visual observations, the addition of protein to alginate improved the film stability in water. Alginate films immediately dissolved after exposure to water, while alginate-protein films remained partially soluble for wheat proteins concentrations of 4 and 6%. Al/WP8 did not dissolve. This result also confirms the improved interactions, mainly of electrostatic nature, between Al and WP, particularly for the highest concentration of WP, which could favour stronger interactions and lower film solubility. The lower film solubility was also observed for fish myofibrillar protein films prepared with higher protein content (Kaewprachu et al., 2016).

3.2.7. *Water vapor transmission rate (WVTR)*

The WVTR of the Al and Al/WP films is shown in Fig. 4C. The WVTR of Al films were approximately 50% lower than other alginate/glycerol films with similar concentration (Miller et al., 2021). It can be noted how the incorporation of proteins substantially increases the WVTR of the films from 124 g m^{-2} day^{-1} (Al films), to 308–194 (Al/WP films), which depended on the concentration of WP solutions. This is likely due to the increased content of the plasticizer (glycerol) which is associated to an increased WVTR (Jost et al., 2014). However, the gradual increase in WP concentration, gradually decreased the WVTR from 308 to 194 g/mm^2/day, respectively. This could have been probably due to the increase in the electrostatic interactions between alginate and the protein at higher protein concentrations, as confirmed by FTIR (Fig. 2) and subsequent compaction of the structure (less porous) (Fig. 3), which offers higher resistance to water transport, as also seen in water solubility studies (Table 2).

Many packaging applications require low WVTR as possible, however, some specific applications require breathable packaging, for instance, to minimize the anaerobiosis derived from CO_2 accumulations or steam release in microwaved food.(Kim & Seo, 2018) Herein, it is shown that Al/WP films WVTRs can be adjusted to suit the food just by changing the WP concentration.

3.2.8. *Mechanical properties*

The tensile strength and elongation at break of Al and Al/WP films are displayed in Table 1. The tensile test was used to measure the tensile strength, and elongation at break in the longitudinal direction of the films (Comaposada et al., 2015).

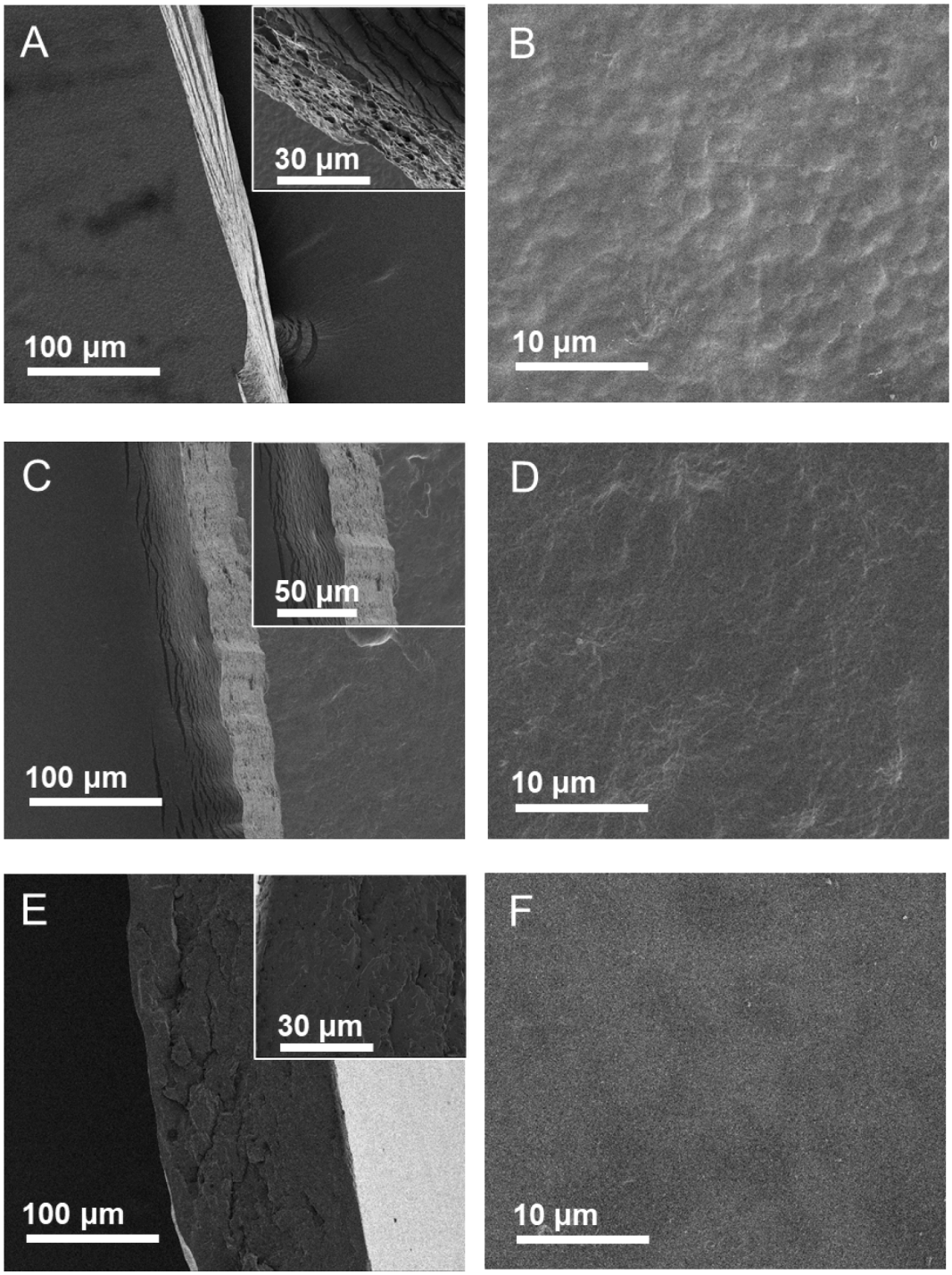

Fig. 3. SEM images of the cross sections (left) and surfaces (right) of Al (A, B), Al/WP4 (C, D) and Al/WP8 (E, F) films. Magnification: 1000x, photos A-F; 5000x, insert in the photos A and E; and 2500x, insert in the photo C.

WP/Al films could not be produced without a plasticizer, and thus glycerol (extensively used in other biopolymer films) was used as plasticizer to contribute to the formation of smoother, more flexible and stable films(Buffo & Han, 2005)(Gontard et al., 1993)(Farahnaky et al., 2013).

Alginate/glycerol films produced in this study display 11.7 MPa and 17.3% of tensile strength and elongation at break, respectively (Table 1). This is less than calcium alginate/glycerol films prepared by (Barbut & Harper, 2019) which displayed tensile strength of 15–34 MPa and elongation at break of 25–44 %. The superior properties are attributed to the crosslinking with calcium ions. However, the Al/WP4 films showed much lower tensile properties (0.9 MPa of tensile strength and 2.1 MPa of young modulus) than Al films, but also lower tensile properties comparatively to Al/WP6 and Al/WP8 making composites more suitable as edible coating.

Films produced with WP of 6 and 8%.w/v showed tensile strength around 1.2 and 2 MPa respectively. The increase of the TS with increase of protein concentration from 4 to 8 %.w/v was not statistically significant ($p > 0.05$). Studies of commercial, soft and hard wheat proteins films cast from water/ethanol solvent mixtures solutions have been showing tensile strength ranging from 0.29 to 0.57 (commercial); 0.24–0.34 (soft films) and 1.2–1.57 (hard films) MPa respectively

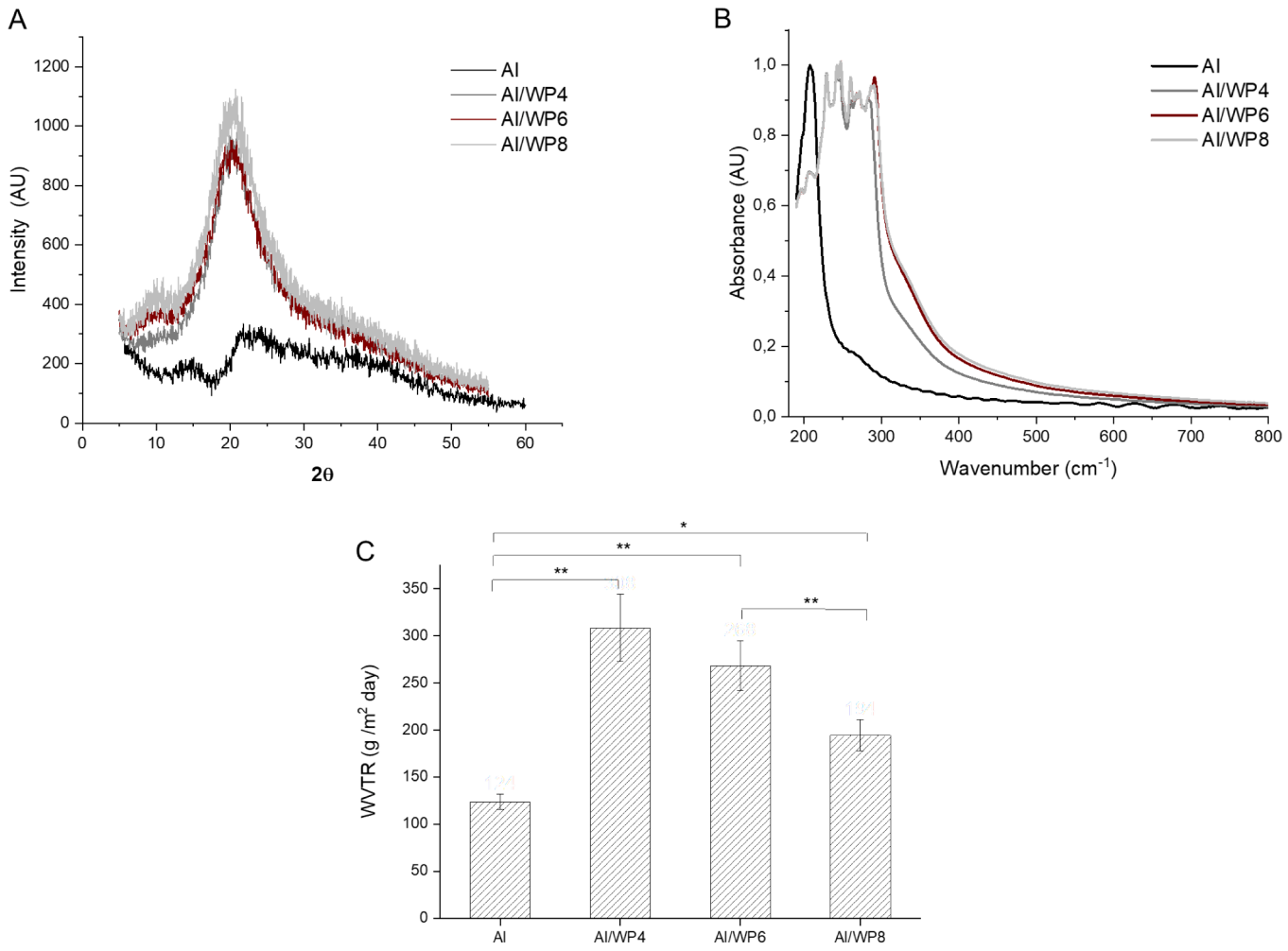

Fig. 4. XRD (A); UV–Vis spectra (B) and WVTR of Al, AL/WP4; Al/WP6 and Al/WP8 films. (N = 3).

Table 1
Thickness, transparency, colour parameters* and mechanical properties of Al and Al/WP films (N = 3).

Sample	Thickness (mm)	Transparency	L	a	b	ΔE	Young's modulus (MPa)	Tensile strength (MPa)	% Elongation at break
Al	0.048 ± 0.0	27,8	−0.97 ± 0.2	0.08 ± 0.1	1.84 ± 0.4	2.11 ± 0.4	61.7 ± 6.4	11.7 ± 2.1	17.3 ± 2.1
Al/ WP4	0.162 ± 0.0[a]	10,5[a]	1.13 ± 1.1	−0.85 ± 0.1[c]	0.66 ± 0.4[b]	1.90 ± 0.4	2.1 ± 0.5[a]	0.9 ± 0.2[b]	37.8 ± 5.1[a]
Al/ WP6	0.143 ± 0.0[a,f]	12,5[e]	3.41 ± 1.1[b,e]	0.90 ± 0.2[a,d]	9.25 ± 1.4[a,d]	9.92 ± 1.7[a,d]	2.5 ± 0.6[a]	1.2 ± 0.5[b]	44.6 ± 11[a]
Al/ WP8	0.136 ± 0.0[a,f]	13,5[e]	4.73 ± 1.4[b,e]	1.08 ± 0.3[a,e]	9.96 ± 0.8[a,d]	11.14 ± 1[a, d]	3.31 ± 0.4[a,e]	2.0 ± 0.2[b,f]	61.6 ± 12[a,d]

a, b, c represent statistical significance P < 0.001 (***), P < 0.01 (**) and P < 0.05 (*) respectively in comparison to Al and similarly d, e, f represent statistical significance P < 0.001 (***),P < 0.01 (**) and P < 0.05 (*) in comparison Al/WP4.

Table 2
Water solubility of Al, Al/WP4, Al/WP6 and Al/WP8 films at room temperature (22 °C) and 90 °C.

Sample	22 ℃	90 ℃
Al	Soluble	Soluble
AL/WP4	Partially soluble	Soluble
AL/WP6	Partially soluble	Soluble
AL/WP8	Not soluble	Partially soluble

(Mojumdar et al., 2011). The films Al/WP displayed a slightly higher TS than the individual commercial wheat films mentioned above, particular for higher concentrations of WP. The relatively lower young modulus and tensile strength values are relevant for applications that require films to protect the foods with similar mechanical properties. Examples include fruits like apples that can have elastic modulus ranging from 0.48 to 1.43 MPa(Masoudi et al., 2008). Furthermore, still in food likes apples the stress value of the films should not be superior to the stress value of the apple, otherwise the deformation of the apple can be accelerated due to induced mechanical damage(Li et al., 2018).

In Table 1 it can also be seen that alginate films displayed the lowest

elongation at break (about 17.3%). Al/WP4 displayed an elongation at break of 37.8%, which tended to increase with the increase of the protein concentration up to 61.6 % for Al/WP8 films ($P < 0.01$). The increase of both tensile strength and elongation at break with the increase of protein concentration was observed, and it has been documented as well for other protein films (e.g. fish myofibrillar protein films, skin gelatin and gelatin film from beef) due to the increase of intermolecular interactions (Kaewprachu et al., 2016).

4. Conclusions

Adjustable polysaccharides-proteins films made of aqueous wheat proteins and alginate solutions were developed by solvent casting. Wheat proteins dispersed in acidic pH were positively charged, as confirmed by zeta potential, which allowed superior interactions with the negatively charged alginate. The interactions of alginate with wheat proteins affected the microstructure, resulting in a higher compaction of the microstructure. Al/WP films showed higher barrier property against UV light, and higher elongation at break and resistance to water, comparatively to the alginate individual films. The concentration of wheat proteins was observed to play an important role to adjust some of the Al/WP film properties, so the films can suit different types of foods and applications. Individual wheat proteins films could not be produced using the described methodology, and individual alginate films using this method could not withstand water. Thus, it is confirmed the relevance of producing polyelectrolyte films of polysaccharides and proteins to improve water insolubility and other properties. The Al/WP films developed in this study, from aqueous biopolymer solutions, with adjustable properties, provide new insights for further uses of wheat proteins, which is a major by-product in the cereal industry. The methodology developed in this study uses a "greener" approach, by using only water as solvent, which might suit a broader range of applications, industries and consumers. Those films have the potential to be used in food applications (e.g. coatings and packaging) that require edible, disposable, UV-light protection properties, and require similar mechanical properties of soft foods like fruits and veggies.

CRediT authorship contribution statement

Shahana Bishnoi: Conceptualization, Methodology, Validation, Formal analysis. **Jon Trifol:** Methodology, Validation, Writing – original draft, Writing – review & editing. **Rosana Moriana:** Writing – review & editing. **Ana C. Mendes:** Conceptualization, Formal analysis, Investigation, Writing – original draft, Writing – review & editing, Supervision, Project administration, Funding acquisition.

Declaration of Competing Interest

The authors declare that they have no known competing financial interests or personal relationships that could have appeared to influence the work reported in this paper.

Acknowledgements

This work was supported by Innovation Fund Denmark (project number 8062-01318B). Ana C. Mendes also thanks to PROBIO project from Innovation Fund Denmark (project number 7076-00053B). John Trifol acknowledges the financial support from the Academy of Finland's Flagship Programme under Projects No. 318890 and 318891 (Competence Center for Materials Bioeconomy, FinnCERES).

References

A. Pascall, M., & Lin, S.-J. (2013). The Application of Edible Polymeric Films and Coatings in the Food Industry. *Journal of Food Processing & Technology*, *04*(02). Doi: 10.4172/2157-7110.1000e116.

Ali, Y., Ghorpade, V. M., & Hanna, M. A. (1997). Properties of thermally-treated wheat gluten films. *Industrial Crops and Products, 6*(2), 177–184. https://doi.org/10.1016/S0926-6690(97)00216-1

Barbut, S., & Harper, B. A. (2019). Dried Ca-alginate films: Effects of glycerol, relative humidity, soy fibers, and carrageenan. *Lwt, 103*(January), 260–265. https://doi.org/10.1016/j.lwt.2019.01.004

Buffo, R. A., & Han, J. H. (2005). Innovations in Food Packaging. In J. H. Han (Ed.), *Innovations in Food Packaging* (pp. 277–300). Academic Press. https://doi.org/10.1016/B978-012311632-1/50049-8.

Chakravartula, S. S. N., Soccio, M., Lotti, N., Balestra, F., Dalla Rosa, M., & Siracusa, V. (2019). Characterization of composite edible films based on pectin/alginate/whey protein concentrate. *Materials, 12*(15), 1–19. https://doi.org/10.3390/ma12152454

Chinabhark, K., Benjakul, S., & Prodpran, T. (2007). Effect of pH on the properties of protein-based film from bigeye snapper (Priacanthus tayenus) surimi. *Bioresource Technology, 98*(1), 221–225. https://doi.org/10.1016/j.biortech.2005.11.012

Comaposada, J., Gou, P., Marcos, B., & Arnau, J. (2015). Physical properties of sodium alginate solutions and edible wet calcium alginate coatings. *LWT - Food Science and Technology, 64*(1), 212–219. https://doi.org/10.1016/j.lwt.2015.05.043

Csapó, J., Prokisch, J., Albert, C., & Sipos, P. (2019). Effect of UV light on food quality and safety. *Acta Universitatis Sapientiae, Alimentaria, 12*(1), 21–41. https://doi.org/10.2478/ausal-2019-0002

Day, L., Augustin, M. A., Batey, I. L., & Wrigley, C. W. (2006). Wheat-gluten uses and industry needs. *Trends in Food Science and Technology, 17*(2), 82–90. https://doi.org/10.1016/j.tifs.2005.10.003

Diaz-Montes, E., & Castro-Muñoz, R. (2021). Edible Films and Coatings as Food-Quality Preservers: An Overview. *Foods*, *10 (2)*(249), 1–26. Doi: 10.3390/foods10020249.

Farahnaky, A., Saberi, B., & Majzoobi, M. (2013). Effect of glycerol on physical and mechanical properties of wheat starch edible films. *Journal of Texture Studies, 44*(3), 176–186. https://doi.org/10.1111/jtxs.12007

Ganzevles, R. A., Kosters, H., Van Vliet, T., Stuart, M. A. C., & De Jongh, H. H. J. (2007). Polysaccharide charge density regulating protein adsorption to air/water interfaces by protein/polysaccharide complex formation. *Journal of Physical Chemistry B, 111*(45), 12969–12976. https://doi.org/10.1021/jp075441k

Garg, S., Cran, M. J., & Mishra, V. K. (2019). Effect of heating and acidic pH on characteristics of wheat gluten suspension. *International Journal of Food Science and Technology, 54*(5), 1892–1900. https://doi.org/10.1111/ijfs.14097

Gontard, N., Guilbert, S., & Cuq, J. (1993). Water and Glycerol as Plasticizers Affect Mechanical and Water Vapor Barrier Properties of an Edible Wheat Gluten Film. *Journal of Food Science, 58*(1), 206–211. https://doi.org/10.1111/j.1365-2621.1993.tb03246.x

Jost, V., Kobsik, K., Schmid, M., & Noller, K. (2014). Influence of plasticiser on the barrier, mechanical and grease resistance properties of alginate cast films. *Carbohydrate Polymers, 110*, 309–319. https://doi.org/10.1016/j.carbpol.2014.03.096

Kaewprachu, P., Osako, K., Benjakul, S., & Rawdkuen, S. (2016). Effect of protein concentrations on the properties of fish myofibrillar protein based film compared with PVC film. *Journal of Food Science and Technology, 53*(4), 2083–2091. https://doi.org/10.1007/s13197-016-2170-7

Kim, D., & Seo, J. (2018). A review: Breathable films for packaging applications. *Trends in Food Science & Technology, 76*, 15–27. https://doi.org/10.1016/j.tifs.2018.03.020

Langstraat, T. D., Jansens, K. J. A., Delcour, J. A., Puyvelde, P. V., & Goderis, B. (2015). Controlling wheat gluten cross-linking for high temperature processing. *Industrial Crops and Products, 72*, 119–124. https://doi.org/10.1016/j.indcrop.2014.11.058

Li, Y., Du, X., Wang, J., & Lei, C. (2018). Study on mechanical properties of apple picking damage. *Advances in Engineering Research, 120*, 1666–1670. https://doi.org/10.2991/ifeesm-17.2018.304

Liu, C., & Ma, X. (2016). Study on the mechanism of microwave modified wheat protein fiber to improve its mechanical properties. *Journal of Cereal Science, 70*, 99–107. https://doi.org/10.1016/j.jcs.2016.05.018

Lowry, G. V., Hill, R. J., Harper, S., Rawle, A. F., Hendren, C. O., Klaessig, F., … Rumble, J. (2016). Guidance to improve the scientific value of zeta-potential measurements in nanoEHS. *Environmental Science: Nano, 3*(5), 953–965. https://doi.org/10.1039/c6en00136j

Masoudi, H., Tabatabaeefar, A., & Borghaee, A. M. (2008). Investigation on mechanical properties of apples during storage using penetration test. *International Journal of Agriculture and Biology, 10*(1), 69–72.

Mendes, A. C., & Pedersen, G. A. (2021). Perspectives on sustainable food packaging:– is bio-based plastics a solution? *Trends in Food Science & Technology, 112*, 839–846. https://doi.org/10.1016/j.tifs.2021.03.049

Mendes, A., Sevilla Moreno, J., Hanif, M., Douglas, E. L., Chen, M., & Chronakis, I. (2018). Morphological, Mechanical and Mucoadhesive Properties of Electrospun Chitosan/Phospholipid Hybrid Nanofibers. *International Journal of Molecular Sciences, 19*(8), 2266. https://doi.org/10.3390/ijms19082266

Miller, K., Silcher, C., Lindner, M., & Schmid, M. (2021). Effects of glycerol and sorbitol on optical, mechanical, and gas barrier properties of potato peel-based films. *Packaging Technology and Science, 34*(1), 11–23. https://doi.org/10.1002/pts.2536

Mohamed, S. A. A., El-Sakhawy, M., & El-Sakhawy, M. A. M. (2020). Polysaccharides, Protein and Lipid -Based Natural Edible Films in Food Packaging: A Review. *Carbohydrate Polymers, 238*, Article 116178. https://doi.org/10.1016/j.carbpol.2020.116178

Mojumdar, S. C., Moresoli, C., Simon, L. C., & Legge, R. L. (2011). Edible wheat gluten (WG) protein films. *Journal of Thermal Analysis and Calorimetry, 104*(3), 929–936. https://doi.org/10.1007/s10973-011-1491-z

Mozafarpour, R., Sedaghat, N., & Alhasan, F. (2021). Improvement the barrier and mechanical properties of whey protein isolate film using fructan obtained from Serish (Eremurus spectabilis) root as a novel polysaccharide. *Journal of Food*

Measurement and Characterization, 15(2), 1774–1784. https://doi.org/10.1007/s11694-020-00784-8

Otoni, C. G., Avena-Bustillos, R. J., Azeredo, H. M. C., Lorevice, M. V., Moura, M. R., Mattoso, L. H. C., & McHugh, T. H. (2017). Recent Advances on Edible Films Based on Fruits and Vegetables—A Review. *Comprehensive Reviews in Food Science and Food Safety, 16*(5), 1151–1169. https://doi.org/10.1111/1541-4337.12281

Parreidt, T. S., Müller, K., & Schmid, M. (2018). Alginate-based edible films and coatings for food packaging applications. *Foods, 7*(10), 1–38. https://doi.org/10.3390/foods7100170

Rhim, J.-W. (2004). Physical and mechanical properties of water resistant sodium alginate films. *LWT - Food Science and Technology, 37*(3), 323–330. https://doi.org/10.1016/j.lwt.2003.09.008

Rojas-Lema, S., Nilsson, K., Trifol, J., Langton, M., Gomez-Caturla, J., Balart, R., … Moriana, R. (2021). Faba bean protein films reinforced with cellulose nanocrystals as edible food packaging material. *Food Hydrocolloids, 121*, Article 107019. https://doi.org/10.1016/j.foodhyd.2021.107019

Salama, H. E., Abdel Aziz, M. S., & Sabaa, M. W. (2018). Novel biodegradable and antibacterial edible films based on alginate and chitosan biguanidine hydrochloride. *International Journal of Biological Macromolecules, 116*, 443–450. https://doi.org/10.1016/j.ijbiomac.2018.04.183

da Silva, M. A., Bierhalz, A. C. K., & Kieckbusch, T. G. (2009). Alginate and pectin composite films crosslinked with Ca2+ ions: Effect of the plasticizer concentration. *Carbohydrate Polymers, 77*(4), 736–742. https://doi.org/10.1016/j.carbpol.2009.02.014

Skendi, A., Zinoviadou, K. G., Papageorgiou, M., & Rocha, J. M. (2020). Advances on the Valorisation and Functionalization of By-Products and Wastes from Cereal-Based Processing Industry. *Foods, 9*(9), 1243. https://doi.org/10.3390/foods9091243

Tong, Z., Chen, Y., Liu, Y., Tong, L., Chu, J., Xiao, K., … Chu, X. (2017). Preparation, Characterization and Properties of Alginate/Poly(γ-glutamic acid) Composite Microparticles. *Marine Drugs, 15*(4), 91. https://doi.org/10.3390/md15040091

Trifol, J., van Drongelen, M., Clegg, F., Plackett, D., Szabo, P., & Daugaard, A. E. (2019). Impact of thermal processing or solvent casting upon crystallization of PLA nanocellulose and/or nanoclay composites. *Journal of Applied Polymer Science, 136*(20), 47486. https://doi.org/10.1002/app.47486

Trifol, J., Marin Quintero, D. C., & Moriana, R. (2021). Pine Cone Biorefinery: Integral Valorization of Residual Biomass into Lignocellulose Nanofibrils (LCNF)-Reinforced Composites for Packaging. *ACS Sustainable Chemistry & Engineering, 9*(5), 2180–2190. https://doi.org/10.1021/acssuschemeng.0c07687

Wrolstad, R. E., & Smith, D. E. (2017). Color Analysis. In *Food Analysis, Food Science Text Series* (pp. 545–555). © Springer International Publishing 2017 545. https://doi.org/10.1007/978-3-319-45776-5_31.

Zhang, C., Wang, Z., Li, Y., Yang, Y., Ju, X., & He, R. (2019). The preparation and physiochemical characterization of rapeseed protein hydrolysate-chitosan composite films. *Food Chemistry*, *272*(August 2018), 694–701. Doi: 10.1016/j.foodchem.2018.08.097.

Zhang, Z., Zhang, R., Zou, L., & McClements, D. J. (2016). Protein encapsulation in alginate hydrogel beads: Effect of pH on microgel stability, protein retention and protein release. *Food Hydrocolloids, 58*, 308–315. https://doi.org/10.1016/j.foodhyd.2016.03.015